Experimental study on shear strength behavior and numerical study on geosynthetic-reinforced cohesive soil slope

Waqas Hassan[1] · Badee Alshameri[1] · Muhammad Naqeeb Nawaz[1] · Sana Ullah Qamar[1]

Abstract

The successful application of geosynthetic reinforcement in granular soil motivates additional research into the practicality of geosynthetics in cohesive soils. The shear strength behavior of three different cohesive soils (non-, low, and medium plastic) was investigated with two types of geosynthetics (woven geotextile (WGT) and geogrid (GG)) by executing a series of triaxial compression tests with and without reinforcement. Additionally, slope stability analyses on reinforced earth slope were carried out utilizing the limit equilibrium (LE) (Slide and Slope/W), finite element (FE) (PLAXIS), and ordinary method of slices approach (analytical). The experimental results revealed that WGT was found to be more effective than GG due to higher interface friction resistance and tensile strength. The escalation in shear strength was observed 241% and 140% with four layers of WGT and GG, respectively. However, the reinforcement was found to be more efficient in non-plastic soil compared with low and medium-plastic soils in gaining shear strength. The rise in shear strength with WGT was observed 241%, 121%, and 89%, respectively, for non-, low-, and medium-plastic soils. These results indicate that strong WGT–clay interaction existed for non-plastic soil, while a weak WGT–clay interaction exists for other soil. Furthermore, FE analysis yields lower values of factor of safety than the LE analysis. The safety factor values computed from Slope/W are in excellent agreement with analytical results of LE method than Slide software. In conclusion, FEM is found to be more reliable for soil–structure interaction phenomenon which involves complex stress–strain behaviors.

Introduction

Geosynthetics are broadly employed in geotechnical engineering and play a substantial role in the stability of many construction projects such as the construction of roads, embankments over weak soil, retaining walls, and steep slopes [1–3]. Geosynthetic materials upsurge the shear strength (SS) of the soil mass by supplying tensile strength, interface friction resistance, and reducing the lateral deformation of soil [4, 5]. Geosynthetics are widely used to reinforce the soil retaining structures instead of steel because of their flexibility, durability, higher resistance to chemical degradation and corrosion, cost-effectiveness, and fast construction rate. Reinforcing steep slopes is a primary application of geosynthetics [6–8].

Nowadays, for soil improvement, geosynthetic practice to reinforce the soils has become a more habitually used process than other improvement techniques such as chemical stabilization and densification methods [9–11]. Earlier studies endorse that granular soil has been efficaciously reinforced with geosynthetic materials, which encourages further investigation to examine the consequences of geosynthetic reinforcing cohesive soil [12]. Most of the previous works were carried out in the past to investigate the effectiveness of geosynthetic reinforcement on the SS of coarse-grained soil. Chen et al. [13] documented that the

✉ Waqas Hassan
waqashasan65@gmail.com;
whassan.phd19nice@student.nust.edu.pk

Badee Alshameri
badee.alshameri@yahoo.com; b.alshameri@nice.nust.edu.pk

Muhammad Naqeeb Nawaz
naqeebnawaz32@gmail.com;
mnawaz.ms19nice@student.nust.edu.pk

Sana Ullah Qamar
sanaullahuet978@gmail.com;
Sullah.ms19nice@student.nust.edu.pk

1   National University of Sciences and Technology, Islamabad, Pakistan

provision of three layers of GG reinforcement in mudstone coarse-grained soil results in an 18.5% lift in apparent cohesion and a 32% upsurge in the frictional angle. Denine et al. [14] reported a 100 to 150% rise in SS and the cohesion value of sandy soil with the addition of two geotextile layers. Parihar and Shukla [15] proclaimed that a 131% gain in the unconfined compressive strength has been observed with the embodiment of three geotextile layers. Numerous investigators have examined the effectiveness of geosynthetic-reinforced sand using direct shear, triaxial, and unconfined compression tests, and the outcomes reveal that the insertion of reinforcement in sandy soil increased the SS [16–20]. Latha and Murthy [21] declare that gaining the SS of soil planer reinforcement layers less effective than a cellular form of reinforcement. Naeini et al. [22] investigated the behavior of the shear strength of GG-reinforced silty sand and reported a significant enhancement in the shear strength of the soil. Nguyen et al. [23] studied the performance of sand reinforced with non-woven geotextile through a triaxial compression test and reported that geotextile increases the shear strength significantly after deformation of 1–3% axial strain. Alshameri et al. [24, 25] and Alshameri [26] studied the influences of density, fines, and moisture content on the shear strength parameters of sand–kaolin mixture. Al-Subari et al. [27] examined the impact of steel, polypropylene, and coir geosynthetic reinforcement on the bearing capacity of strip footing in sandy soil. Their results showed that coir geosynthetic reinforcement was more effective than other reinforcements in gaining shear strength and bearing capacity. Badakhshan and Noorzad [28] and Dastpak et al. [29] analyzed the influence of eccentricity loading and shape of footing on the bearing capacity of a foundation rested on a sand bed reinforced with geosynthetic. Mudgal et al. [30] executed several triaxial tests on WGT and non-woven-reinforced sand and documented that the WGT reinforcement exhibited adequate improvement in strength while non-woven geotextile showed better interlocking.

There is not much research available on the reinforcing of fine-grained soil with geosynthetics in the literature. Carlos et al. [31] examined the feasibility and improved the SS and California bearing ratio of cohesive soil with multiple layers of geocomposite reinforcement. Their results showed an enhancement in strength of cohesive soil with the inclusion of geocomposite. Malik et al. [32] strengthened the bearing capacity of the shallow footings by stabilizing the soft clay with the addition of granular material. Portelinha et al. [33] reported that non-woven geotextile reinforcement effectively enhanced the SS of fine-grained soil. Shukla et al. [34] studied the effectiveness of woven and non-woven geotextile reinforcement in sandy clay. Their results showed that a 60% and 64% upsurge in SS of sandy clay was observed with inclusion of three layers of non-woven and woven geotextile, respectively. Karakan [35] investigated the consequence of various factors that affect the SS of compacted clay reinforced with geotextile and reported that non-woven geotextile-reinforced clay showed plastic behavior than unreinforced clay. Some studies investigate the combined effect of stabilization and geosynthetic reinforcements. Jayawardane et al. [36] inspected the combined influence of geotextile reinforcement and fly ash to enhance the strength characteristics of cohesive soil. Jahandari et al. [37] studied the collective outcome of lime and GG reinforcement to enhance the geotechnical properties of clayey soil. They reported a 31–78% rise in unconfined compression strength of clay with the application of both lime and geogrid. Jahandari et al. [38] documented that the enhancement in unconfined compression strength with lime and geogrid is two times higher than the increase with lime alone, at a curing period of 365 days. Vajrala and Yenigalla [39] stated that the geosynthetics reinforcement effectively increased the bearing capacity of soft compressible clayey soil and helped reduce the thickness of pavement layers. Karim et al. [40] examined the behavior of soft clay with stabilization of fly ash and reinforcement of GG. According to their findings, adding fly ash also lowers settlement by up to 40–50% while soft clay settlement is claimed to decrease with an increase in the reinforcement layer. However, the previous research has not adequately examined the impact of various geosynthetic reinforcement types on the SS performance of various cohesive soil types (i.e., non-plastic, low, and medium plastic).

Furthermore, geosynthetic soil reinforcement is regarded as a practical method for enhancing earth slopes, embankments, earthen dams, and earth retaining structures [41]. Geotextiles cause an increase in the safety factor of the slopes [42, 43]. In geotechnical engineering, both the limit equilibrium (LE) concepts and the finite element (FE) method have been used for the assessment of the reinforced slope stability [44, 45]. A well-known method for examining slope stability is LE, which involves slicing slopes into finite slices and using the relevant equilibrium equations. Depending on the type of problem and anticipated accuracy, many LE-based approaches have been developed [46]. In contrast to FE analysis, which uses constitutive models or stress–strain relationships, the LE approach works with the static equilibrium of forces. For modeling reinforced slopes, finite element analysis is a new method being used in geotechnical engineering. The construction process, material reinforcement, and complex geometry can all be accurately modeled using FE techniques. In general, FE analysis is more intricate than LE. However, its outcomes and related safety factor are more precise and practical [47]. The strength reduction (SRM) approach is the most often utilized methodology in FE for slope stability [48, 49]. The key advantage of SRM is that a crucial slip circle is discovered automatically, and PLAXIS software is utilized for FE-based slope analysis [43, 44].

Bergado et al. [50] studied to evaluate the geotextile performance on the slope stability of embankments using numerical analysis by PLAXIS software. Cheng et al. [48] compared the safety factors of slopes obtained by LE and FE methods using PLAXIS and Slope/W programs. Olia et al. [51] studied the response of 10 m and 20 m high ground anchored walls under different Loading by applying a numerical model prepared by the finite difference method. Koca and Koca [52] performed the comparative analysis of FE and LE approaches for slope stability analysis of fractured rock slopes using PHASE and Slide software. Their results revealed that significant difference in FOS values exist for both LE and FE methods. Many researchers have performed the FE analysis for geotextile-reinforced slopes [53–56]. Some researchers presented the comparison between LE and FE method for unreinforced earth slope, and some stated that the LE approach is better, and some are in the favors of the FE approach [44, 57, 58]. Senapati and Senapati [60] compared the factor of safety values of slopes using LE and FE methods. Their results indicate that LEM yields higher safety factors values and noteworthy difference exist between safety factors values obtained from FEM and LEM approaches. In light of literature review, it can be concluded that there is a need to explore the reasons behind the significant variance among the factor of safety values obtained from LEM and FEM approaches in slopes reinforced with geotextiles using different software. Additionally, Cheng et al. [61] stated that significant variation in factor of safety values exists from various commercial computer programs. The researchers are yet to confirm the most reliable analysis techniques between LEM and FEM. Therefore, this study aim is to explore the most reliable commercial computer program for the assessment of slope stability using various techniques, i.e., LEM, FEM.

In the field, the usual practice is to use high-quality granular materials in the reinforced structure, but the high-quality materials are not easily obtainable all the time or costly. Sometimes, locally available soil can be used without negotiating serviceability and durability. Most of the existing studies are on coarse-grained soil, and very few studies are available on cohesive soils. Almost all earlier studies have examined the behavior of geosynthetics in one type of cohesive soil. A very limited studies are available in which SS behavior of low-plastic and medium-plastic clay was investigated with geosynthetic reinforcement. However, the effect of different types of geosynthetic reinforcement on the shear strength behavior of non-plastic, low-plastic, and medium-plastic cohesive soil has not been addressed properly in the literature. The beneficial effect of using geosynthetics in different cohesive soil is not identical. It is required to investigate which type of cohesive soil will be more suitable for geosynthetic reinforcement when the option is only cohesive soil at the site. Therefore, the first

objective of this study is to examine the effects of two types of geosynthetic reinforcement (i.e., woven geotextile and geogrid) on the shear strength behavior of three types of cohesive soils by performing a series of triaxial compression tests. Moreover, the second objective of this study is to explore the most trustworthy technique among LEM and FEM for the stability analysis of reinforced slopes. For this, the slope stability analysis of reinforced embankments has been carried out through analytical and numerical methods. This study utilizes two commercial tools based on the LE approach (Slope/W and Slide), and their reliability has been judged by comparing the results with analytical calculations, while FE analysis has been performed using PLAXIS 2D software. Slides 6.0 and Slope/W are used for LE analysis, while PLAXIS 2D is for FE analysis.

Materials used

Soils samples

To analyze the consequence of soil plasticity on the geosynthetics-reinforced soil, the three naturally available cohesive soil samples were gathered from distinct sites and designated as S0, S5, and S11. The numbers (0, 5, and 11) represented the plasticity indexes of each soil. Particle size analysis has been performed on the three soil samples, and the particle gradation curves are depicted in Fig. 1. According to the results, the mean particle size (D_{50}) of the soil is 0.05, 0.025 and 0.01 mm, respectively, for S0, S5, and S11soil. The S0 sample is non-plastic, S5 is low-plastic, and the S11 soil sample is slightly medium-plastic. The samples are classified as sandy silt (ML), clayey silt (CL-ML) and silty clay (CL) as per the Unified Soil Classification System (USCS). The standard and modified proctor tests have been executed to
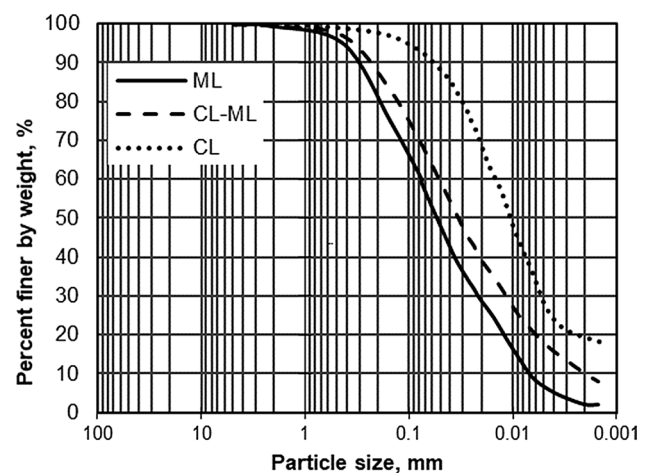

Fig. 1 Grain size distributions curves

determine the maximum dry density and optimum moisture content for each soil. The index and compaction properties are outlined in Table 1.

Reinforcement samples

Two types of geosynthetic reinforcements (GG and WGT) are used in this research to investigate the consequence of reinforcements on the SS of cohesive soils and to analyze the stability of reinforced earth slopes. Both reinforcement materials were collected from Zhejiang Chengmei Co., Ltd China. WGT is made of polyester, while the GG employed in this work is an extruded polymer net made of high-density polyethylene (HDPE) with an aperture size of 6.0 mm square. The tensile strength of both materials is equal in the longitudinal and transverse directions since they are both biaxial. Table 2 provides a summary of the mechanical and physical characteristics of geosynthetics as determined by ASTM standards. Mass per unit area, thickness, and specific gravity are the physical properties of geosynthetics and determined by following their ASTM standards [62, 63], whereas tensile strength is the mechanical property of geosynthetics material and determined by following their ASTM standard [64]. Figure 2 expresses the stress–strain behavior of geosynthetics material which indicates WGT has higher tensile strength than GG material.

Methodology

This study has been divided into two parts: In part 1, an experimental study was executed to examine the SS behavior of three different types of cohesive soil with two different kinds of geosynthetics reinforcement. However, in part 2, the numerical analysis was carried out to explore the most trustworthy technique among LEM and FEM for the analysis of reinforced earth slopes. The general methodology of the current study is shown in Fig. 3.

Experimental study

A total of 45 unconsolidated undrained (UU) triaxial compression tests were executed to examine the influences of geosynthetics reinforcement on the SS behavior of varying plasticity cohesive soils. In addition, various tests were repeated during the experiments to sure the accuracy of the results. These tests were carried out on a cylindrical specimen of unsaturated soil with and without reinforcement. Several remolded soil specimens of a diameter of 76.2 mm with a height to diameter ratio of 2 were prepared in the laboratory by following the moist temping method as per standard [65]. In the past, most of the earlier studies were performed on a specimen size of 38 to 100 mm diameter

Table 1 Basic properties of soil samples

Soil (#)	L.L (%)	P.I (%)	G_S (−)	D_{50} (mm)	Sand (%)	Silt (%)	Clay (%)	Standard proctor		Modified Proctor		USCS/AAHSTO
								$\rho_{d,max}$ (g/cc)	OMC (%)	$\rho_{d,max}$ (g/cc)	OMC (%)	
S0	18	N.P	2.60	0.05	40	58	2	1.62	15.5	1.78	13.0	ML/A-4(0)
S5	24	5	2.67	0.025	31	59	10	1.56	17.8	1.72	14.2	CL-ML/A-4(5)
S11	30	11	2.70	0.01	7	73	20	1.51	18.7	1.68	16.1	CL/A-6 (15)

Table 2 Physical and mechanical properties of geosynthetic

Materials	Mass par unit area (g/m^2)	Thickness (mm)	Effective opening size (mm)	Specific gravity	Ultimate tensile strength (kN/m)	Axial strain at failure (%)	Elastic modulus, E$_{50}$ (MN/m)
WGT	300	0.35	0.3	1.30	86	17.52	4.5
GG	530	2.8	6.0	0.90	35	60	4.3
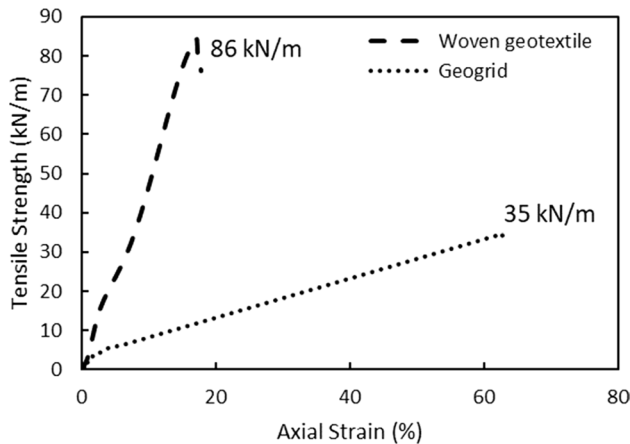
Fig. 2 Stress–strain behavior of geosynthetic materials

[14, 36, 66, 67]. To ensure the consistency of test results, the techniques for specimen preparation and testing were standardized. All the preliminary tests were replicated until consistency in the results was obtained. The reinforcement layers arranged horizontally, and the schematic sketch of reinforcement is illustrated in Fig. 4. These tests were performed under cell pressures of 30, 40, and 50 kPa and strain rate of 1%/min kept constant in all tests as recommended by ASTM [65] for cohesive soils. Moreover, for triaxial compression tests of reinforced soil, the employed strain rates range was 1 to 1.5%/mm by various researchers [21, 23, 68]. The low confining pressure in the specimen testing was taken to represent the actual field condition of the embankment because in the case of the embankment, the lateral pressure is quite low. Air was used for confining pressure, and tests were executed following ASTM [65]. All the remolded soil specimen was compacted to a modified proctor density and corresponding moisture content. For reinforcement layers, geosynthetic material was cut into a circular disk form having a diameter size of 73 mm, as shown in Fig. 3.

Numerical study

In part 2, the slope stability analysis of reinforced embankment slope was executed by analytical and numerical approach using different commercially available software (i.e., GeoStudio (Slope/W), PLAXIS, and Slide) to compare the results between LE and FE methods. For the analytical approach, the ordinary method of slices was used. This approach was based on the LE concept [5]. Both Slide 6.0 and Slope/W have been used for LE analysis, while PLAXIS-2D V8 has been used for FE analysis. The Mohr–Coulomb failure criterion was used to model the embankment slope, and the material parameters of the soil are depicted in Fig. 10. On a modeled embankment slope, both with and without numerous layers of reinforcement, the slope stability analysis was performed. The reinforcement was positioned horizontally at intervals ranging from H/2 to H/8, where H is the embankment height. Under the assumption of a critical circular failure plane, the slope stability analysis was executed for six slices in terms of total stresses. For LE analysis, the tensile strength and interface frictional properties of geosynthetic reinforcement are considered for simulation in Slide and Slope/W [69]. The slope was modeled in PLAXIS 2D for FE analysis. Plain strain model was adopted with Mohr–Coulomb model as a material model which required cohesion (*c*), friction angle (*φ*), elastic modulus (*E*), Poisson's ratio, and unit weight. The material characteristics provided in Tables 1, 2 were determined through laboratory testing and used for simulation. The medium-coarse mesh was used considering the conditions, and to perform analysis in PLAXIS 2D, the phi-c (strength reduction) analysis was selected.

Results and discussion

Stress–strain behavior

The deviator stress versus axial strain curves for unreinforced specimens and multiple layers of reinforced specimens were compared to recognize the irrespective change in stress–strain behavior with the addition of WGT and GG reinforcement, as shown in Fig. 5. A surge in deviator stress was observed in reinforced specimens at all confining pressures (30, 40, and 50 kPa) compared with unreinforced specimens because of an increase in internal confinement of soil specimen [67]. At cell pressure of 50 kPa in S0 soil, the maximum increase in peak deviator stress ($\Delta\sigma$) with the addition of WGT reinforcement is observed 50%, 89%, 154%, and 225%, respectively, for
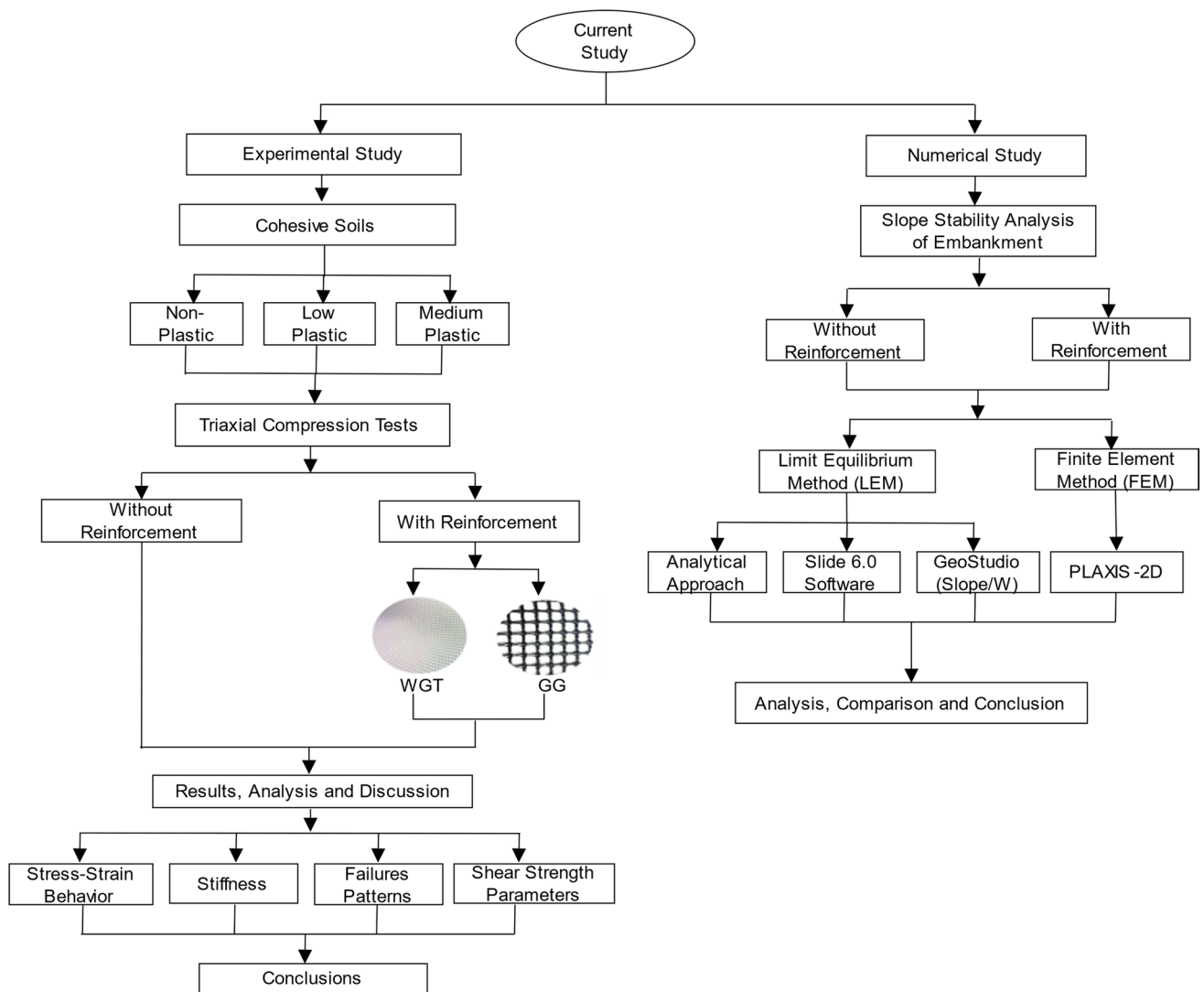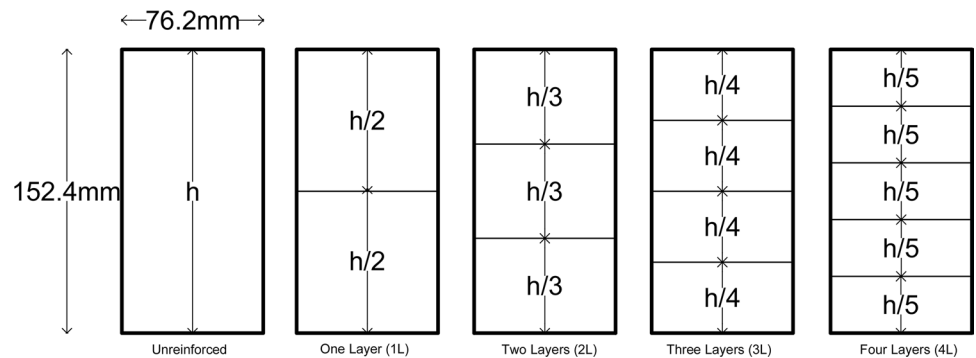
Fig. 3 Methodology and framework of current study

**Fig. 4** Schematic sketch of geosynthetic reinforcement

one, two, three, and four layers. Similarly, with the inclusion of GG reinforcement, the increase in $\Delta\sigma$ is observed 54%, 90%, 161%, and 223%, respectively, for 1, 2, 3, and 4 layers of reinforcement. The reason behind this incremental rise in $\Delta\sigma$ is accredited to the tensile strength of the reinforcement material, which increases, respectively, with the increase in reinforcement layers. Another possible reason for this is that the reinforcement layers may have intercepted the specimen's failure plane, dispersing stresses across the soil in an even manner and thereby enriching
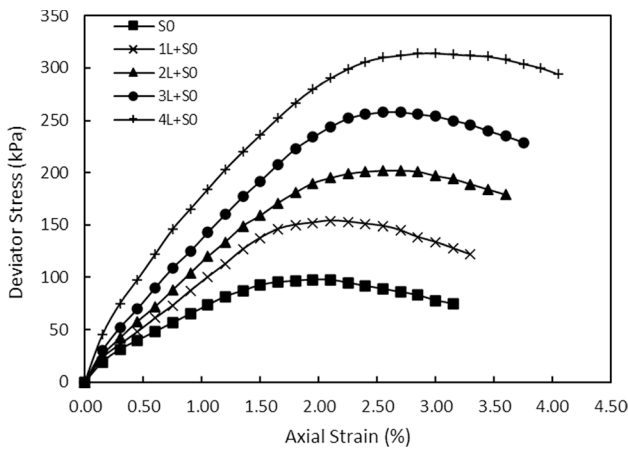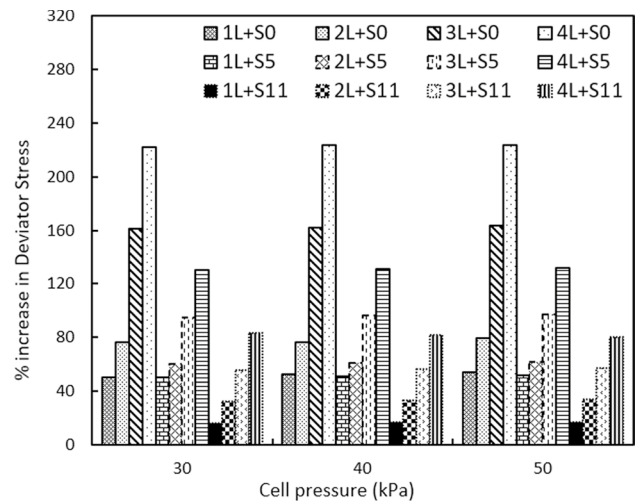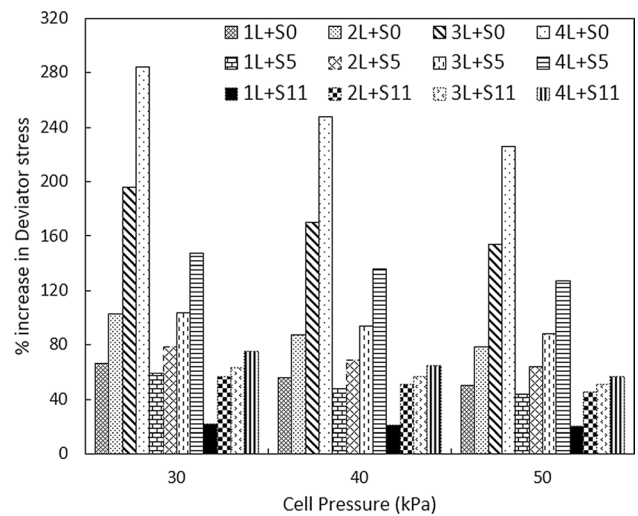
(a) GG Reinforcement
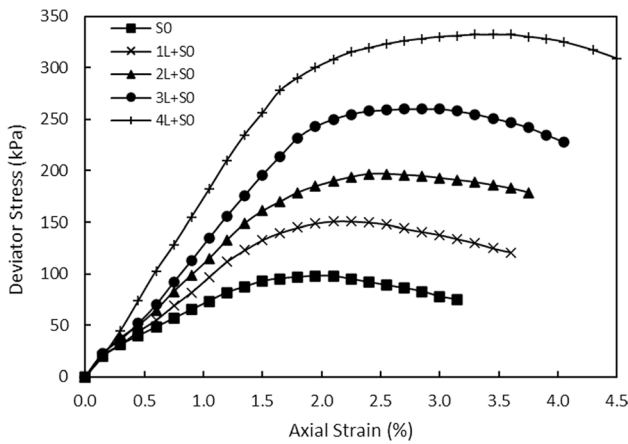
(b) WGT Reinforcement

Fig. 5 Stress–strain behavior of geosynthetic-reinforced S0 Soil

(a) GG Reinforcement

(b) WGT Reinforcement

Fig. 6 Percentage increase in peak deviator stresses

the total strength of the reinforced soil [68]. A comparable trend has been stated by Chen et al. [13] and Naeini et al. [22] that escalation in $\Delta\sigma$ is credited to the tensile strength of reinforcing materials. Similar behavior in sandy soil was also stated by [36, 66, 67]. Figure 5b indicates that due to the compressibility of WGT material at the initial load, there is no substantial increase in deviator stresses up to 0.5% strain after that significant increase was observed. The thickness of the WGT material is reduced initially with a rise in normal load, after it starts to bear loads, as justified by Denine et al. [14] and Carlos et al. [31]. According to Yang et al. [70], the geotextile reinforcement needs enough deformation to mobilize its tensile strength, which subsequently helps the reinforced soil's overall shear strength increase. This result is consistent with the findings of Noorzad and Mirmoradi [68], Fabian and Fourie [71], Yang et al. [70, 72], Ingold and Miller [73], and Unnikrishnan et al. [74] in reinforced clayey soil. Analogous behavior is also observed in S5 and S11 soils with the provision of WGT and GG reinforcement.

The comparison between three soils (S0, S5, and S11) in terms of percentage increases in $\Delta\sigma$ is drawn in Fig. 6. Generally, two trends were observed in percentage increase in $\Delta\sigma$, such as decline and rise, with escalation of cell pressure. In the case of GG reinforcement, the percentage increase in $\Delta\sigma$ value is slightly increased with the rise in cell pressure, as shown in Fig. 6a. For S0 soil with the addition of four layers of GG (4L + S0), the increase in $\Delta\sigma$ is observed 222%, 223%, and 224%, respectively, at cell pressure of 30, 40, and 50 kPa. Similarly, for (4L + S5) soil, the increase in $\Delta\sigma$ is observed 130%, 131%, and 133%. However, the percentage increase in $\Delta\sigma$ is limited to only 82%, 84%, and 85% in case of (4L + S11) soil. It can be noted that the increment of $\Delta\sigma$ in S0 soil is two to three times higher than in S11 soil. The percentage increase in $\Delta\sigma$ is higher in S0 soil than in S5 and S11 soil due to the higher interface frictional resistance

between soil and reinforcement material. The upsurge in the plasticity of the soil results in a decline in interface frictional resistance, which ultimately results in less increase in peak deviator stresses. For (4L + S0) soil with WGT reinforcement, the increase in $\Delta\sigma$ is observed 284%, 248%, and 225%, respectively, at cell pressure of 30, 40, and 50 kPa, as shown in Fig. 6b. Similar behavior has been observed in the case of S5 and S11 soil with WGT reinforcement. The percentage increase in $\Delta\sigma$ is decreasing with a rise in cell pressure is accredited to the poor tensile strength of the WGT material at the high strain that limits the increase in deviator stress. A similar reason for this decrement in $\Delta\sigma$ with the rise in cell pressure has been proclaimed by Denine et al. [14]. Another possible reason behind this decrement is that the increase in cell pressure results in a decrease in an interaction caused between soil and reinforcement material [75]. However, the contradictory behavior has been observed with the inclusion of GG reinforcement which is accredited to the rigidity or non-compressibility of the material and excellent tensile strength of the material at high strain level. WGT and GG are two distinct kinds of reinforcement techniques. WGT reinforcement is a frictional endurance-dependent system in which friction must initiate at the soil–reinforcement interface to preclude sliding, while GG is a passive endurance-dependent system in which stresses from the soil to GG are transmitted via bearing at the soil to the netting crossbar interface. As pressure is applied, soil interlocking between the GG's apertures mobilizes the material's higher tensile strength, and a sufficient anchoring effect has been accomplished [76]. It is shown in Fig. 6 that there was no linear relationship between the increase in deviator stress and the number of reinforcement layers in the reinforced samples. Four-layer reinforcement, in particular, was seen to have caused in a higher gain in deviator stress compared to the one-, two-, and three-layer samples at all cell pressures. It was most likely caused by the addition of a fourth layer for the sample (4L + S0), which resulted in a significant decrease in vertical space between reinforcement layers. Due to the significant reduction in layer space, there might have been "multiple" reinforcing layers present, preventing a critical failure plane and distributing the forces uniformly throughout the soil specimen. However, WGT reinforcement is found to be more effective than GG due to the higher tensile strength and soil–reinforcement interface interaction.

Stiffness

The stiffness in terms of elastic modulus (E_{50}) has been determined from the stress–strain curves of different reinforced soils. It has been noted that an increase in reinforcement layers has caused the soil sample's stiffness to increase, as presented in Fig. 7. The stiffness of soil also rises with the escalation of cell pressure in both unreinforced
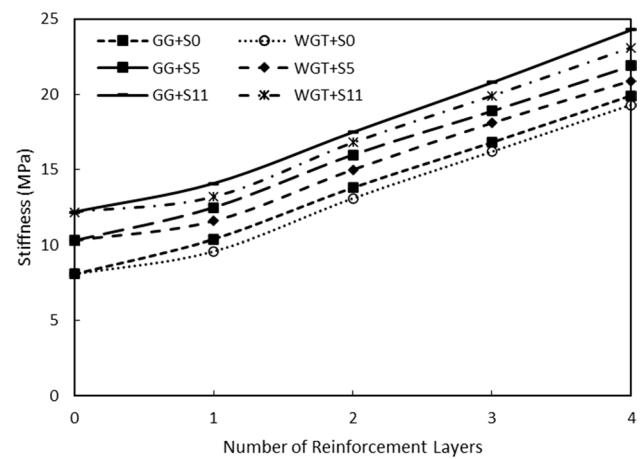

Fig. 7 Effect of reinforcements on stiffness of different reinforced soils at cell pressure of 50 kPa

and reinforced soil. In the case of S0 soil, the surge in stiffness value is observed from 8.1 to 19.9 (146% increase) and 19.3 (138% increase), respectively, with the addition of four layers of GG and WGT reinforcement at a cell pressure of 50 kPa. The stiffness value of S5 soil is increased from 10.3 to 21.9 (113% increase) and 20.9 MPa (102% increase), respectively, for four layers of GG and WGT reinforcement. Similarly, the stiffness value of S11 soil is increased from 12.2 to 24.3 (99% increase) and 23.1 MPa (89% increase), respectively. The tensile strength and interfacial frictional resistance between the soil and substance are likely the causes of this increase [77]. Singh [66] proclaimed that major principle stress has been increased with a rise in cell pressure, which boosts the frictional capability of the reinforcement that increases with an rise in major principle stress. This increase in the frictional capability of reinforcement results in higher stiffness of the reinforced specimen. Comparable outcomes were also documented by Chen et al. [13]. It has been noted that GG reinforcement yields slightly higher stiffness values than WGT reinforcement because of the hardness of the material. Another reason behind this phenomenon is the interlocking of soil particles between the grids of GG reinforcement, as explained by Jayawardane et al. [36]. However, the percentage increase in stiffness values of S0 soil is more than S5 and S11 soil due to the higher interface frictional resistance between the reinforcement and soil. The increase in the plasticity of the soil results in a decrease in interface frictional resistance. The same sort of trends has been observed at a cell pressure of 30 and 40 kPa.

Failure patterns

The failure patterns of the unreinforced and reinforced specimen are demonstrated in Fig. 8. The shear failure has been observed in an unreinforced soil specimen along
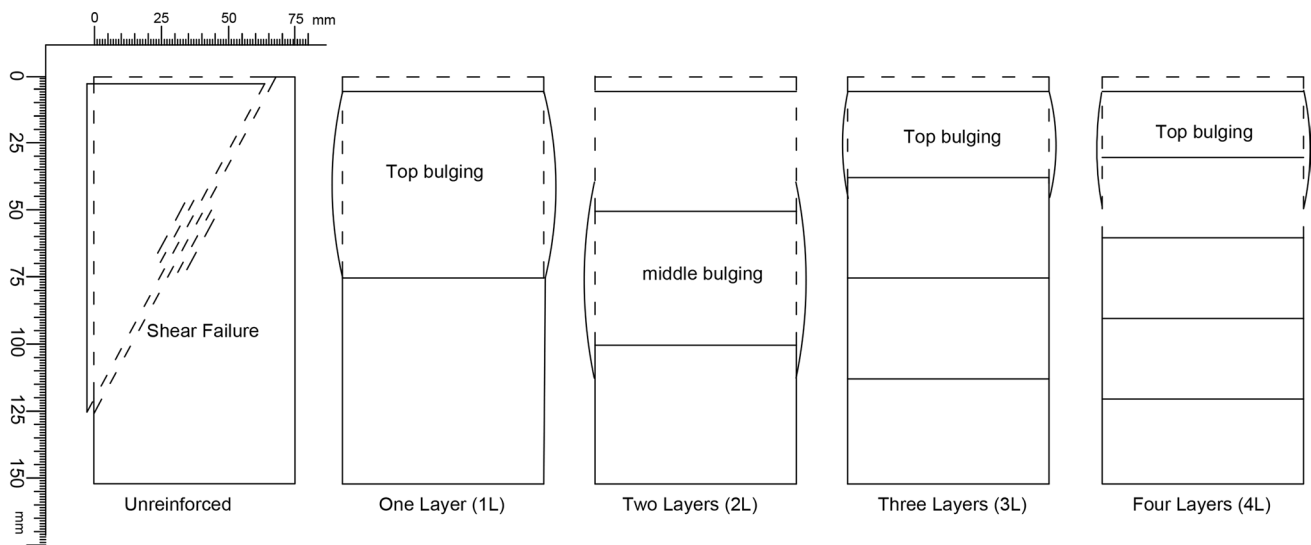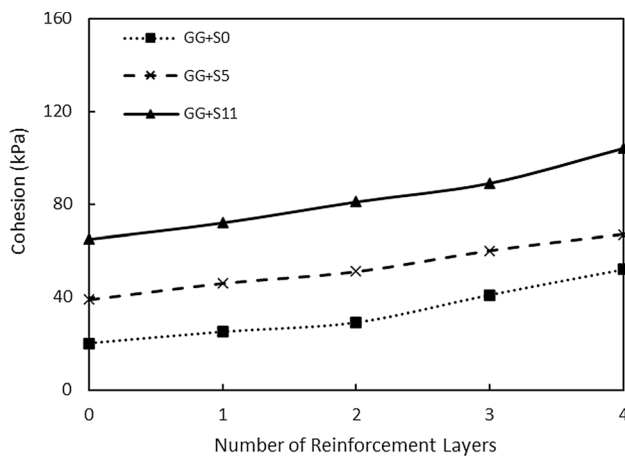
Fig. 8 Failure modes of specimen with different layers of reinforcement
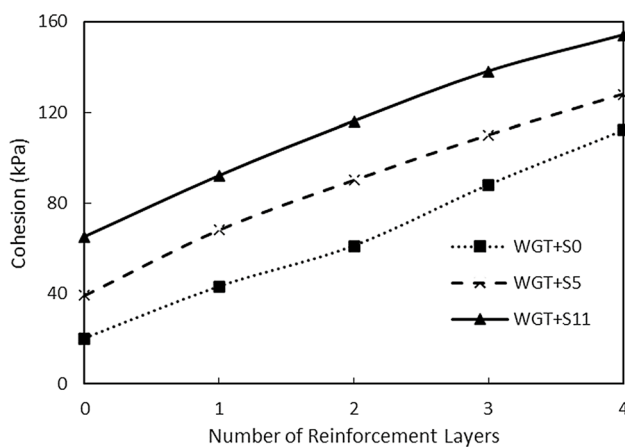
a plane at an angle of $45 + \phi/2$ approximately [67]. Contrastingly, bulging failure has been perceived in the case of reinforced soil specimens. Top bulging failure has seen in single, triple, and four layers of the reinforced soil specimen. However, middle bulging has been seemed in the case of two layers of the reinforced soil specimen. The reinforcement inclusion deprived the soil lateral displacement near the reinforcement area, and therefore, higher displacement appeared between two bordering reinforcement layers. The deformation became relatively homogeneous as the number of geotextile layers rose (less bulging). The homogeneous deformation of a sample indicated that the deployed stresses had been evenly disseminated throughout the soil, thus increasing the shear strength of the reinforced specimen [70]. The bulging failure has been accredited to the increase in confinement of the soil mass [78]. Another plausible logic is the shear resistance of the soil specimen that increases with the provision of reinforcement layers [13]. The reinforcement rises the shear resistance of the specimen by providing additional tensile strength to the soil specimen and reduces the lateral deformation of soil because of interface frictional resistance among the soil and reinforcement materials [79]. Furthermore, the inconsistency in the bulging failure may be accredited to the unequal compaction of soil specimen during its preparation, which may have changed the density of soil in the top and middle layers, which in turn results in middle layer bulging failure [36]. Similar failure patterns were also reported by Jayawardane et al. [36], Yang et al. [70, 72], Fabian and Foure [71], and Sreelakshmi and Vasudevan [80] in reinforced clayey soil. Comparable outcomes were also reported by various researchers in granular soil [14, 21, 77].

Undrained shear strength parameters

WGT and GG reinforcements have a prodigious impact on the strength of the soil, and both reinforcement materials show different behaviors depending on their interaction with soil grains and physical and mechanical properties. To ascertain the parameters cohesion/apparent cohesion and internal angle of friction of unreinforced/reinforced soil, the Mohr–Coulomb failure envelop has been drawn in terms of total stresses. The effect of reinforcements on cohesion/apparent cohesion of different soils (S0, S5, and S11) are presented in Fig. 9a, b. It was noted that the addition of reinforcement layers into soil mass substantially increases the cohesion of soil, and its favorable effect increases with an increase in intensity of reinforcement layers. For S0 soil, the cohesion value has increased from 20 to 52 kPa with the provision of four layers of GG and 20 to 112 kPa with the addition of four layers of WGT reinforcement. The 160% and 460% gain has been observed in apparent cohesion with the provision of four layers of GG and WGT reinforcement, respectively. For S5 soil, the cohesion has increased from 39 to 67 kPa and 39 to 128 kPa, respectively, with the provision of four layers of GG and WGT reinforcement. The incremental rise in apparent cohesion observed 72 and 228%, respectively, for four layers of GG and WGT reinforcement. Similarly, in S11 soil, the cohesion value has risen from 65 to 104 kPa and 65 to 154 kPa, respectively. The incremental increase in apparent cohesion has limited to only 60% and 137%, respectively, for four layers of GG and WGT. However, the percentage increase in apparent cohesion is more in S0 soil compared with S5 and S11 soil because of the nonplasticity of the soil, which in turn results in higher interface frictional resistance between the soil and reinforcement.
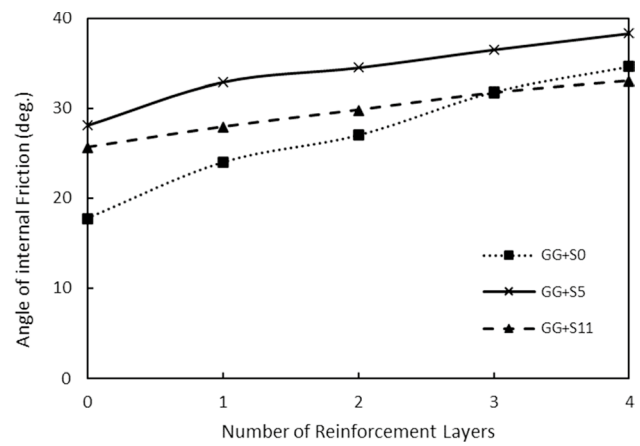
Fig. 9 Effect of reinforcement on cohesion1/apparent cohesion of different soils

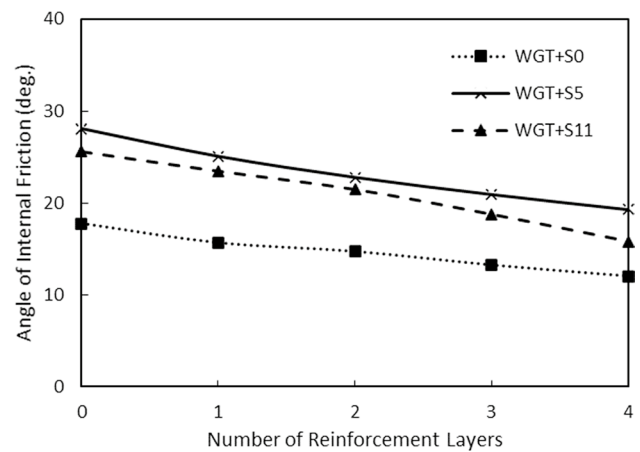**Fig. 10** Effect of reinforcement on frictional angle of different soils

Moreover, WGT reinforcement found to be more effective in gaining apparent cohesion due to the higher tensile strength and higher surface area, which results in higher interface frictional resistance [81].

The improvement in cohesion value is due to various reasons. The probable reason behind this increase in apparent cohesion is the confinement of the soil specimen, which improved with the addition of reinforcement layers [13, 31]. The escalation in apparent cohesion has attributed to the interlocking of reinforcement layers with soil particles; consequently, the no. of interaction points among soil particles was reduced [14]. The apparent cohesion value increases with the provision of reinforcement layers which are due to the material tensile strength and interface frictional resistance that increases proportionally with the reinforcement layers [36, 81]. According to the concept of apparent cohesion, the existence of reinforcement in soil mass increases the major principle stress at failure, which increased the

cohesion value [82]. Another potential reason is the reduction in the build-up of pore water pressure because of the permeability of reinforcement layers. Due to the undrained condition, the pore water pressure would have produced during the deviator stress application. However, as both of the reinforcing materials were porous and permitted drainage, the developed pore water pressure would have dispersed from the sample more quickly than it would have from a sample of unreinforced soil. Larger drainage channels for the dissipation of excess pore water pressure were created by the increase in reinforcing layers, and this, in turn, led to higher effective stresses in the reinforced specimen [71].

The effect of reinforcement on the internal angle of friction of reinforced soil is presented in Fig. 10a, b. It has been observed that the addition of WGT decreases the frictional angle and increases with the provision of GG reinforcement. In S0 soil, the frictional angle has raised from 17.75 to 34.6° (95% increment) and decreases from 17.75 to 12° (32% decrement), respectively, with the provision of four layers of GG

and GTW. Similarly, in S5 and S11 soil, increment in the frictional angle has perceived 72% and 42%, while decrement has been observed 31% and 38%, respectively, with the inclusion of four layers of GG and WGT. Denine et al. [14] and Hassan et al. [81] stated that geotextile decreases the angle of internal friction of soil considerably with escalation in the number of reinforcement layers due to the decrease in direct soil to soil contact. Yang and Singh [83] and Yang [84] reported that reduction in the frictional angle with the provision of geotextile reinforcement has been ascribed to the sliding of soil particles along the geotextile and soil interface. It is conflicting with the assertation of Schlosser and Long [82] and agree with the findings of Yang et al. [70], Iwamoto [85] and Haeri et al. [67]. However, geogrid reinforcement significantly increases the frictional angle due to the interlocking action among the GG reinforcement apertures and soil, and the particles of soils remain in contact with each other, as justify by Jewell et al. [79] and Koernel [5]. Similar results for GG reinforcement have also been reported by various researchers [13, 66, 86]. Moreover, in the WGT reinforcement case, the shear strength chiefly originates from cohesion while from the frictional angle in the GG reinforcement case and the friction angle is the main parameter that contributes to the shear strength of soil because the increase in cohesion is not significant as compared with WGT.

The augmentation in shear strength parameters ultimately increases the shear strength of the soil. The shear strength has been determined against the overburden load of 20 kPa. A comparison among three types of soil and the two types of reinforcement in terms of shear strength is shown in Fig. 11. It has been observed that the shear strength of the soil rises with an rise in reinforcement layers. These findings indicate that the strong reinforcement–clay interaction existed under less reinforcement spacing for S0 soil. Another possible

reason for this is that the reinforcement layers may have intercepted the specimen's failure plane, dispersing stresses across the soil in an even manner and thereby enhancing the total shear strength of the reinforced soil [68]. Nguyen et al. [23] and Yang et al. [72] revealed a direct and linear connection among the mobilized reinforcement tensile strength/load and shear strength enhancement of reinforced soil by experimentally examining the mobilized tensile strain/load of reinforcement. WGT reinforcement found to be more effective than GG in gaining the shear strength due to high tensile strength and higher interface frictional resistance. For example, the escalation in shear strength observed 241% and 140%, respectively, with the addition of four layers of WGT and GG. This result indicates that the strong WGT–clay interaction existed for S0 soil, while a weak GG–clay interaction exists for the same soil. Among the three types of soils, S0 soil is found to be more effective than S5 and S11 soils. For example, percentage increase in shear strength has been observed 241%, 121%, and 89%, respectively, for S0, S5, and S11 soils with the addition of four layers of WGT reinforcement. The possible reason for this is that the strong interface interaction exists between reinforcement and S0 soil rather than S5 and S11 soil. It has been concluded that geosynthetic reinforcement gives highly effective results in non-plastic cohesive soil rather than low- and medium-plastic soil. This observation is agreed with the findings of Noorzad and Mirmoradi [68], Hassan et al. [81], and Fourie and Fabian [87].

Analytical and numerical analysis of reinforced earth slopes

In this section, an attempt has been made for the slope stability analysis of embankment earth slope by four different approaches. The first approach is the analytical, the ordinary

Fig. 11 Effect of reinforcement on shear strength of different soils
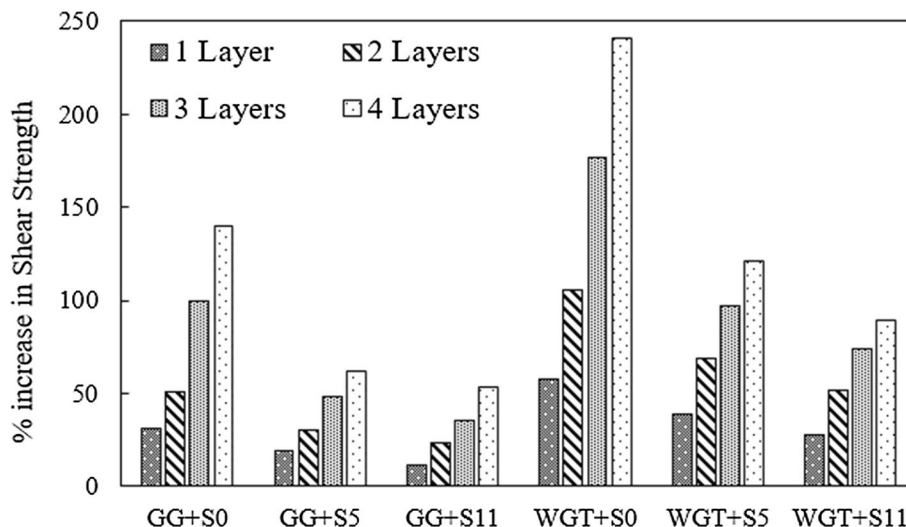
method of slices was used [5], and the remaining three are software's based (i.e., Slide, PLAXIS, and Slope/W). The free-body diagram of the embankment slope is shown in Fig. 12. The slope stability analyses have been performed on the presented embankment slope with and without multiple layers of geosynthetic reinforcement (i.e., WGT and GG). The reinforcement was positioned horizontally at intervals ranging from H/2 to H/8, where H is the embankment height equal to 9.5 m. The single layer has been placed at H/2, the two layers have been placed at H/3, and three layers have been placed at a vertical distance of H/4. Similarly, all other layers are placed at an equal vertical height of the embankment. The angle of the slope from the horizontal earth surface is 50°, and the properties of the embankment and foundation soil are shown in Fig. 12.

In geotechnical engineering, usually, the limit equilibrium concept on a supposed circular arc failure plane is used for slope stability related problems. The factor of safety in terms of total stress has been determined using Eq. (1).

$$\text{F.O.S} = \frac{F_R}{F_D} = \frac{\left(cR\theta + \tan\phi \times \sum N\right)R + \sum T_{all} \sum * y_i}{R \cdot \sum T} \quad (1)$$

where F_R and F_D are resisting and disturbing force, respectively, T_{all} is the allowable tensile strength of geosynthetic, y_i is the moment arm of reinforcement material, c is the cohesion of the backfill soil, R is the radius of the circular arc, ϕ is the frictional angle of the backfill soil, N is the normal force acting perpendicular to the sliding surface, and T is the shear force acting parallel to the sliding surface. Due to its ease of use, this strategy is frequently employed in practice. The properties of geosynthetic materials are shown in Table 2. Allowable tensile strength has been calculated by

assuming an overall reduction factor of 0.35 for the long-term performance of reinforcement materials. The tensile strength of geosynthetic materials decreases due to damages during installation, creep effect, and chemical and biological degradation [5]. The allowable tensile strength of the materials has been determined as 30 and 12.6 KN/m, respectively, for WGT and GG reinforcement against a reduction factor of 0.35.

The analysis's findings, which are represented in Fig. 13, demonstrate that the factor of safety (FOS) against circular failure planes has grown as a result of adding more reinforcement layers to embankment slopes. The increase in FOS is a result of more layers of reinforcement, and more layers of reinforcement result in a rise in the tensile strength of the reinforcement that is proportionate to the number of layers. FOS against circular failure plane without
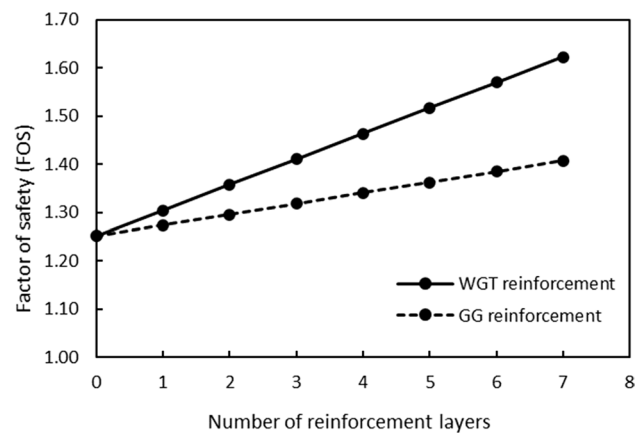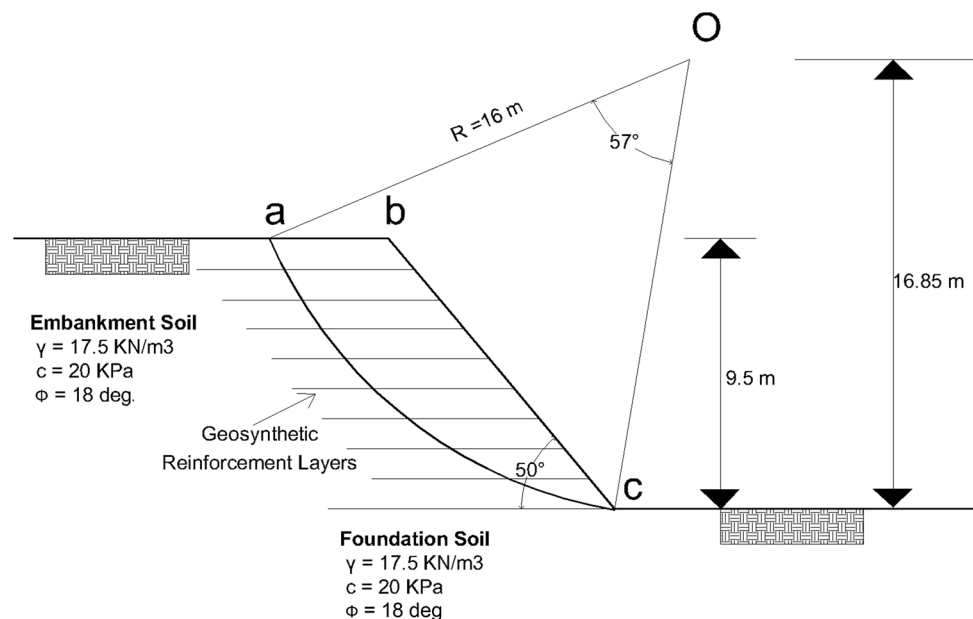

Fig. 13 Slope stability analysis result of analytical approach

Fig. 12 Free-body diagram of Embankment earth slope

reinforcement is 1.25 and increases up to 1.62 with seven reinforcement layers of WGT. Similarly, FOS has increased from 1.25 to 1.41 with seven layers of GG reinforcement. Reinforcement provides additional tensile strength to the soil mass through the mechanism of interlocking and inter-faces frictional resistance [4, 5]. WGT reinforcement shows higher FOS compared with GG reinforcement because of the higher tensile strength of the material. FOS has found to be directly proportional to the quantity of reinforcement lay-ers and tensile strength of the material. From the reinforced embankment analysis, the number of reinforcement layers to be used can be calculated for the desired FOS. For example, to get a FOS of 1.5, one needs to reinforce the embankment with three layers of WGT or more than seven layers of GG.

The same embankment earth slope was modeled in Slide, Slope/W, and in PLAXIS 2D with the material properties presented in Table 2. The reinforcement was done in a simi-lar way as done in analytical analysis. Reinforcement layers were placed horizontally varying from a vertical distance of H/2 to H/8, where H is the embankment height. The Slide, Slope/W, and PLAXIS 2D model of embankment, respectively, is shown in Figs. 14, 15 and 16. The simulation was carried out using Mohr–Coulomb model in all three software. The geotextiles are modeled using in-built tool of supports in Slide and Slope/W. However, for FEM analysis in PLAXIS 2D, the geotextiles are modeled using the plate element. The coarse medium fine mesh was used for FEM analysis. The strength reduction method (SSR) was then applied to analyze the failure mechanism of the embankment slope. On the other hand, Janbu method was used to analyze the FOS from Slide and Slope/W software.

The FOS calculated from these different approaches with and without WGT reinforcement is shown in Table 3.
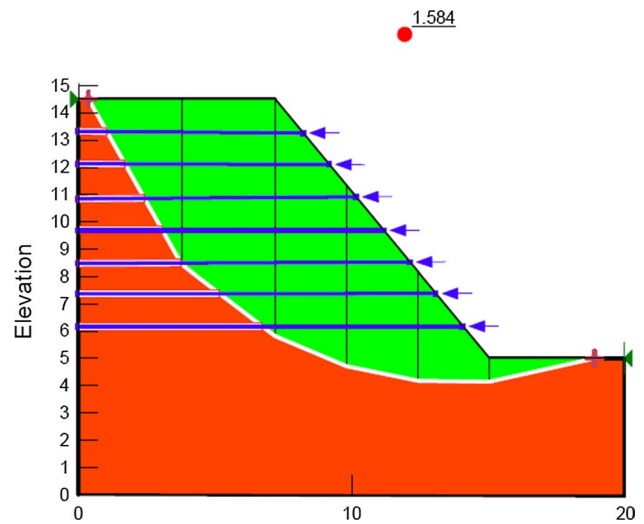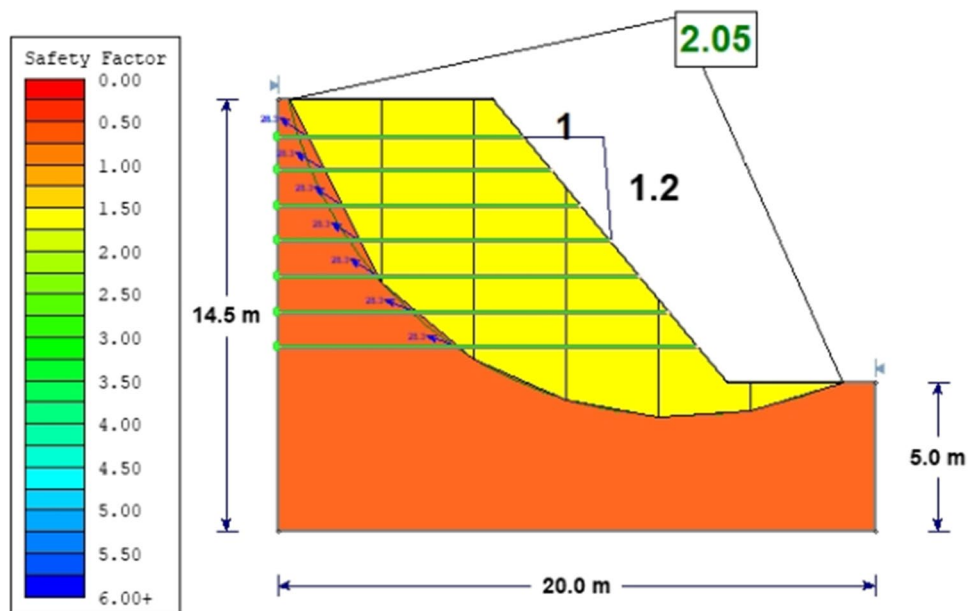

Fig. 15 Embankment earth slope model in Slope/W software

The results of all three software's indicate a considerable increase in FOS with a rise in the amount of reinforcement. That adds to the fact that geotextiles play an imperative role in stabilizing the slopes of an embankment and provide an economical solution to the slopes prone to failure.

A comparison of FOS of embankment slope calculated from analytical, Slide, Slope/W, and PLAXIS 2D methods is shown in Fig. 17. For unreinforced earth slope, determined FOS is almost the same calculated from limit equilibrium (LE) methods while finite element (FE) method gives the lower FOS. Analytical approach, Slope/W, and Slide 6.0 software are LE based while PLAXIS 2D is FE based. The analytical method shows a good agreement with Slope/W results, and FOS are same up to four layers of reinforcement

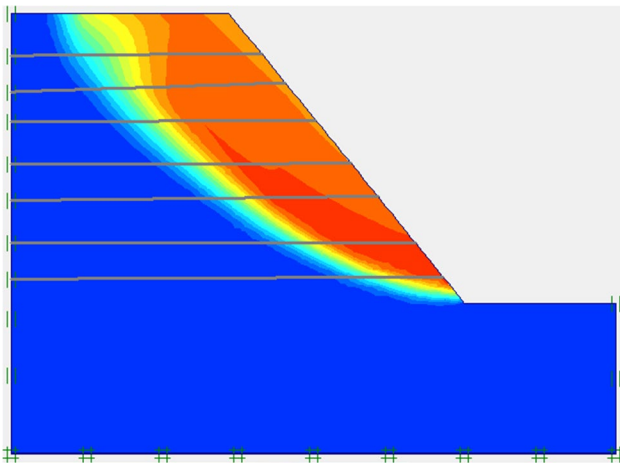**Fig. 14** Embankment earth slope model in slide software

Fig. 16 Embankment earth slope model in PLAXIS 2D software

Table 3 FOS calculated from different methods with and without GTW reinforcement

Number of reinforcement layers	Analytical	Slope/W	Slide 6.0	PLAXIS 2D
0	1.25	1.25	1.24	1.17
1	1.29	1.29	1.33	1.22
2	1.35	1.35	1.43	1.29
3	1.41	1.41	1.51	1.34
4	1.46	1.46	1.59	1.41
5	1.52	1.54	1.64	1.47
6	1.57	1.61	1.72	1.52
7	1.62	1.66	2.05	1.58

then Slope/W gives the slightly higher values of FOS. However, Slide software yields higher values of FOS. FE analysis based on the strength reduction method (phi-c) yields lower values of FOS than other methods and attribute to the fact that the finite element analysis considers the stress and strains at different points and the stiffness and poison ratio of soil. LE-based methods did not consider the stiffness and Poisson's ratio of soil. Another plausible reason that attributes is the critical slip circle that passes through the toe of the embankment with the provision of reinforcement in FE analysis, while it extends beyond the toe of the embankment in LE analyses. The larger slip circle represents a higher weight of soil wedge, which will lead to the fact that a higher amount of driving force is required to produce shear failure. In short, the greater the radius of the slip circle higher the will be a resisting force, and higher will be a factor of safety [57]. Also, in LE methods using Slide and Slope/W tool, the failure geometry is assumed, i.e., (circular slip) prior to analysis. However, in FEM analysis, the SSR method searches out the critical slip surface automatically [88]. Another reason regarding the difference in FOS values is as mentioned in the literature that LEM-based programs do not consider the distribution of overburden [89]. Cheng et al. [61] also mentioned that difference in FOS values obtained from different LEM- and FEM-based program is obvious and certain and also exact reason is yet to be explored. Additionally, Slope/W produces superior outcomes for the LE approach compared to Slide software. However, Slope/W and Slide are regarded as inferior to FEM, and comparable outcomes were also provided by [90]. He claimed that PLAXIS-based software for FEM produces superior outcomes to LEM-based software. Similarly, [90] compared LEM and FEM utilizing Slope/W and PLAXIS to examine the safety factor in toll road embankment slope. They concluded that FEM-based approach yields more realistic results. This in turn

Fig. 17 Comparison of FOS from different methods
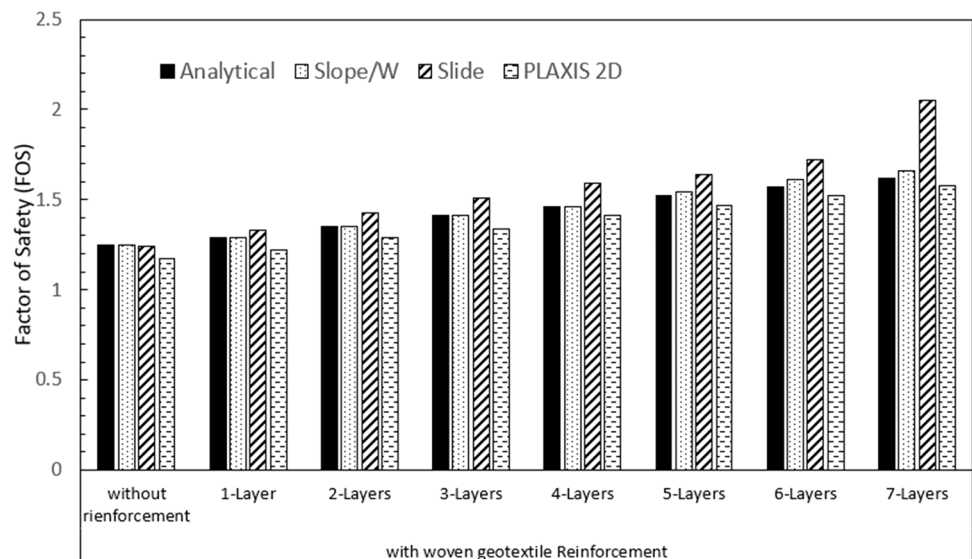
justifies that the current study is in line with the previous findings and provides guides for engineers working in the field to adopt more reliable numerical tool for practice. The aim of comparing both FEM and LEM approaches using different commercially available software was to highlight the variation in factor of safeties for a geotextile-reinforced embankment using different approaches. According to the results of the current investigation, Slope/W produces superior results for the LE approach than Slide. However, Slope/W results also diverge from the analytical approach for a more complex occurrence, such as the reinforcement of more than four geotextile layers in a slope. Due to the complexity of the stress–strain behavior of reinforced slopes, basic LEM-based techniques fall short. Strength reduction method (FEM methodology) is therefore viewed as more realistic and trustworthy in such a scenario.

Conclusions

The shear strength behavior of three different cohesive soils has been investigated with the provision of WGT and GG reinforcements in this study. Moreover, the slope stability analysis of reinforced embankment was carried out with four different methods to explore the most reliable technique among LEM and FEM. Experimental results revealed significant improvement in soil stiffness, angle of internal friction, apparent cohesion, and shear strengths with reinforcements inclusion. It has been accredited to the interlocking, frictional resistance between the soil–reinforcement interface, the tensile strength of the materials, and the increase in the confinement of soil specimens. WGT was found to be more effective than GG due to higher tensile strength and interface friction resistance. For example, 241% and 140% increase in shear strength were observed with four layers of WGT and GG reinforcements, respectively. However, the reinforcement was found to be more efficient in non-plastic soil compared with low-plastic and medium-plastic soils in gaining shear strength. For example, the increase in shear strength with WGT was observed 241%, 121%, and 89%, respectively, for non-, low-, and medium-plastic soils. Results indicate that a strong WGT–clay interaction existed for non-plastic soil, while a weak WGT–clay interaction exists for the low and medium-plastic soil. From this, it can be concluded that higher plastic soil will be less effective in gaining the shear strength with geosynthetics reinforcement. Moreover, for the slope stability analyses, the LE method obtained from Slope/W tools is found to be more reliable than Slide software and is ordinarily in excellent agreement with the results of the analytical approach. The FE analysis (PLAXIS 2D) yields a lower factor of safety than the LE analysis. In conclusion to numerical analysis, FEM-based approach is more reliable for a complex phenomenon that involves stress–strain behavior of soil–structure interaction such as the one discussed in this study.

Despite the fact that experimental outcomes show emphatic effects regarding the shear strength improvement of cohesive soils with reinforcements, the laboratory scales may limit the results, like the size of the soil specimen or dimensions of the testing apparatus. Therefore, it has been recommended to execute experiments on a broader scale by using a larger size sample simulating the field conditions. It has also recommended studying the long-term performance of reinforced cohesive soil by incorporating consolidation and seasonal variations of moisture content.

Declarations

Conflict of interest The author declares that there is no conflict of interest regarding the publication of this article.

Consent of publication The work titled "Experimental study on shear strength behavior and numerical study on geosynthetic-reinforced cohesive soil slope" has not been published elsewhere, in part, or in another form.

References

1. Holtz RD, Shang JQ, Bergado DT (2001) Soil improvement. Geotechnical and geoenvironmental engineering handbook. Springer, Boston, pp 429–462
2. Pinto MIM (2003) Applications of geosynthetics for soil reinforcement. Proc Inst Civ Eng Gr Improv 7:61–72. https://doi.org/10.1680/grim.2003.7.2.61
3. Rowe RK, Taechakumthorn C (2011) Design of reinforced embankments on soft clay deposits considering the viscosity of both foundation and reinforcement. Geotext Geomembr 29:448–461
4. Jewell RA (1996) Soil reinforcement with geotextiles
5. Koernel RM (2005) Design with geosynthetics, 5th edn. Prentice Hall, New Jersey
6. Hawk B, Wu JTH, Wu JTH (2008) Investigating failure of a geosynthetic-reinforced soil wall in black hawk, colorado. In: Presented at the sixth international conference on case histories in geotechnical engineering, Arlington, VA. pp 0–12
7. Shukla SK, Sivakugan N, Das BM (2011) A state-of-the-art review of geosynthetic-reinforced slopes. Int J Geotech Eng 5:17–32. https://doi.org/10.3328/IJGE.2011.05.01.17-32
8. Wu H, Yao C, Li C et al (2020) Review of application and innovation of geotextiles in geotechnical engineering. Materials (Basel) 13:1–21. https://doi.org/10.3390/MA13071774
9. Alibolandi M, Moayed RZ (2015) Liquefaction potential of reinforced silty sands. Int J Civ Eng 13:195–202. https://doi.org/10.22068/IJCE.13.3.195

10. Talamkhani S, Naeini SA (2021) The undrained shear behavior of reinforced clayey sand. Geotech Geol Eng 39:265–283. https://doi.org/10.1007/s10706-020-01490-4

11. Hassan W, Ahmad M, Farooq A et al (2017) Correlation of maximum laboratory dry density and optimum moisture content of soil with soil parameters. NFC-IEFR J Eng Sci Res 5:1–6. https://doi.org/10.24081/nijesr.2016.1.0003

12. Abu-Farsakh M, Coronei J, Tao M (2007) Effect of soil moisture content and dry density on cohesive soil-geosynthetic interactions using large direct shear tests. J Mater Civ Eng 19:540–549. https://doi.org/10.1061/(ASCE)0899-1561(2007)19

13. Chen X, Zhang J, Li Z (2014) Shear behaviour of a geogrid-reinforced coarse-grained soil based on large-scale triaxial tests. Geotext Geomembr 42:312–328. https://doi.org/10.1016/j.geotexmem.2014.05.004

14. Denine S, Della N, Muhammed RD et al (2016) Effect of geotextile reinforcement on shear strength of sandy soil: laboratory study. Stud Geotech Mech 38:3–13. https://doi.org/10.1515/sgem-2016-0026

15. Parihar NS, Shukla RP (2015) Unconfined compressive strength of geotextile sheets reinforced soil. Int J Earth Sci Eng 8:1379–1385

16. Naeini SA, Gholampoor N (2014) Cyclic behaviour of dry silty sand reinforced with a geotextile. Geotext Geomembr 42:611–619. https://doi.org/10.1016/j.geotexmem.2014.10.003

17. Consoli NC, Vendruscolo MA, Fonini A, Rosa FD (2009) Fiber reinforcement effects on sand considering a wide cementation range. Geotext Geomembr 27:196–203. https://doi.org/10.1016/j.geotexmem.2008.11.005

18. Liu J, Feng Q, Wang Y et al (2017) The effect of polymer-fiber stabilization on the unconfined compressive strength and shear strength of sand. Adv Mater Sci Eng 2017:1–9. https://doi.org/10.1155/2017/2370763

19. Hamidi A, Hooresfand M (2013) Effect of fiber reinforcement on triaxial shear behavior of cement treated sand. Geotext Geomembr 36:1–9. https://doi.org/10.1016/j.geotexmem.2012.10.005

20. Plácido R, Portelinha FHM, Futai MM (2018) Field and laboratory time-dependent behaviors of geotextiles in reinforced soil walls. Geosynth Int 25:215–229. https://doi.org/10.1680/jgein.18.00003

21. Latha GM, Murthy VS (2007) Effects of reinforcement form on the behavior of geosynthetic reinforced sand. Geotext Geomembr 25:23–32. https://doi.org/10.1016/j.geotexmem.2006.09.002

22. Naeini SA, Khalaj M, Izadi E (2013) Interfacial shear strength of silty sand-geogrid composite. Proc Inst Civ Eng Geotech Eng 166:67–75. https://doi.org/10.1680/geng.10.00118

23. Nguyen MD, Yang KH, Lee SH et al (2013) Behavior of non-woven-geotextile-reinforced sand and mobilization of reinforcement strain under triaxial compression. Geosynth Int 20:207–225. https://doi.org/10.1680/gein.13.00012

24. Alshameri B, Madun A, Bakar I (2017) Assessment on the effect of fine content and moisture content towards shear strength. Geotech Eng J SEAGS AGSSEA 48:76–86

25. Alshameri B, Madun A, Bakar I (2017) Comparison of the effect of fine content and density towards the shear strength parameters. Geotech Eng J SEAGS AGSSEA 48:104–110

26. Alshameri B (2020) Maximum dry density of sand–kaolin mixtures predicted by using fine content and specific gravity. SN Appl Sci 2:1–7. https://doi.org/10.1007/s42452-020-03481-9

27. Al-Subari L, Hanafi M, Ekinci A (2020) Effect of geosynthetic reinforcement on the bearing capacity of strip footing on sandy soil. SN Appl Sci 2:1–11. https://doi.org/10.1007/s42452-020-03261-5

28. Badakhshan E, Noorzad A (2017) Effect of footing shape and load eccentricity on behavior of geosynthetic reinforced sand bed. Geotext Geomembr 45:58–67. https://doi.org/10.1016/j.geotexmem.2016.11.007

29. Dastpak P, Abrishami S, Sharifi S, Tabaroei A (2020) Experimental study on the behavior of eccentrically loaded circular footing model resting on reinforced sand. Geotext Geomembr 48:647–654. https://doi.org/10.1016/j.geotexmem.2020.03.009

30. Mudgal A, Sarkar R, Shrivastava AK (2018) Influence of geotextiles in enhancing the shear strength of Yamuna sand. Int J Appl Eng Res 13:10733–10740

31. Carlos DM, Pinho-lopes M, Lopes ML (2016) Effect of geosynthetic reinforcement inclusion on the strength parameters and bearing ratio of a fine soil. Procedia Eng 143:34–41. https://doi.org/10.1016/j.proeng.2016.06.005

32. Malik ZB, Alshameri B, Jamil SM, Umar D (2021) Experimental and numerical modeling of bearing capacity of foundations on soft clay stabilized with granular material. Int J Geosynth Gr Eng. https://doi.org/10.1007/s40891-021-00334-2

33. Portelinha FHM, Bueno BS, Zornberg JG (2013) Performance of nonwoven geotextile-reinforced walls under wetting conditions: laboratory and field investigations. Geosynth Int 20:90–104. https://doi.org/10.1680/gein.13.00004

34. Shukla RP, Parihar NS, Gupta AK (2016) The effect of geotextiles on low plastic sandy clay. In: 6th Asian regional conference on geosynthetics - geosynthetics for infrastructure development, 8-11 November, New Delhi, India. pp 251–259

35. Karakan E (2018) Factors effecting the shear strength of geotextile reinforced compacted clays. Deu Muhendis Fak Fen Muhendis 20:725–742. https://doi.org/10.21205/deufmd.2018206057

36. Jayawardane VS, Anggraini V, Li-Shen AT et al (2020) Strength enhancement of geotextile-reinforced fly-ash-based geopolymer stabilized residual soil. Int J Geosynth Gr Eng 6:1–15. https://doi.org/10.1007/s40891-020-00233-y

37. Jahandari S, Saberian M, Zivari F et al (2019) Experimental study of the effects of curing time on geotechnical properties of stabilized clay with lime and geogrid. Int J Geotech Eng 13:172–183. https://doi.org/10.1080/19386362.2017.1329259

38. Jahandari S, Mojtahedi SF, Zivari F et al (2020) The impact of long-term curing period on the mechanical features of lime-geogrid treated soils. Geomech Geoengin. https://doi.org/10.1080/17486025.2020.1739753

39. Vajrala RK, Yenigalla RV (2019) Comparitive study on effect of diverse geosynthetics and their spacing on soft clayey soil. Int J Recent Technol Eng 8:1480–1484

40. Karim HH, Samueel ZW, Jassem AH (2020) Behaviour of soft clayey soil improved by fly ash and geogrid under cyclic loading. Civ Eng J 6:225–237. https://doi.org/10.28991/cej-2020-03091466

41. Raja MNA, Shukla SK (2021) Experimental study on repeatedly loaded foundation soil strengthened by wraparound geosynthetic reinforcement technique. J Rock Mech Geotech Eng 13:899–911. https://doi.org/10.1016/j.jrmge.2021.02.001

42. Bergado DT, Teerawattanasuk C (2008) 2D and 3D numerical simulations of reinforced embankments on soft ground. Geotext Geomembr 26:39–55

43. Briançon L, Villard P (2008) Design of geosynthetic-reinforced platforms spanning localized sinkholes. Geotext Geomembr 26:416–428

44. Liu SY, Shao LT, Li HJ (2015) Slope stability analysis using the limit equilibrium method and two finite element methods. Comput Geotech 63:291–298

45. Zheng H, Liu DF, Li C (2005) Slope stability analysis based on elasto-plastic finite element method. Int J Numer Methods Eng 64:1871–1888

46. Huang YH (2014) Slope stability analysis by the limit equilibrium method: Fundamentals and methods. American Society of Civil Engineers

47. Li D-Q, Xiao T, Cao Z-J et al (2016) Efficient and consistent reliability analysis of soil slope stability using both limit

equilibrium analysis and finite element analysis. Appl Math Model 40:5216–5229

48. Cheng YM, Lansivaara T, Wei WB (2007) Two-dimensional slope stability analysis by limit equilibrium and strength reduction methods. Comput Geotech 34:137–150

49. Griffiths DV, Lane PA (1999) Slope stability analysis by finite elements. Geotechnique 49:387–403

50. Bergado DT, Long PV, Murthy BRS (2002) A case study of geotextile-reinforced embankment on soft ground. Geotext Geomembr 20:343–365

51. Olia ASR, Oliaei M, Heidarzadeh H (2021) Performance of ground anchored walls subjected to dynamic and pseudo-static loading. Civ Eng J 7:974–987. https://doi.org/10.28991/cej-2021-03091703

52. Koca TK, Koca MY (2020) Comparative analyses of finite element and limit-equilibrium methods for heavily fractured rock slopes. J Earth Syst Sci 129:1–13

53. Hammah RE, Yacoub TE, Corkum BC, Curran JH (2005) The shear strength reduction method for the generalized Hoek-Brown criterion. In: American rock mechanics association - 40th US rock mechanics symposium, ALASKA ROCKS 2005: rock mechanics for energy, mineral and infrastructure development in the northern regions

54. Kanungo DP, Pain A, Sharma S (2013) Finite element modeling approach to assess the stability of debris and rock slopes: a case study from the Indian Himalayas. Nat Hazards 69:1–24. https://doi.org/10.1007/s11069-013-0680-4

55. Griffiths DV, Lane PA (2001) Slope stability analysis by finite elements. Géotechnique 51:653–654. https://doi.org/10.1680/geot.51.7.653.51390

56. Hinchberger SD, Rowe RK (2003) Geosynthetic reinforced embankments on soft clay foundations: predicting reinforcement strains at failure. Geotext Geomembr 21:151–175

57. Alemdag S, Kaya A, Karadag M et al (2015) Utilization of the limit equilibrium and finite element methods for the stability analysis of the slope debris: an example of the Kalebasi District (NE Turkey). J Afr Earth Sci 106:134–146. https://doi.org/10.1016/j.jafrearsci.2015.03.010

58. Alkasawneh W, Husein Malkawi AI, Nusairat JH, Albataineh N (2008) A comparative study of various commercially available programs in slope stability analysis. Comput Geotech 35:387–403. https://doi.org/10.1016/j.compgeo.2007.06.009

59. Salmasi F, Norouzi R, Abraham J et al (2020) Effect of inclined clay core on embankment dam seepage and stability through LEM and FEM. Geotech Geol Eng 38:6571–6586

60. Senapati S, Senapati S (2021) Comparison of LEM and FEM based solution for slope stability analysis using soilworks. In: Advances in Sustainable Construction Materials 2020, vol 124. p 341

61. Cheng YM, Länsivaara T, Wei WB (2008) Reply to "Comments on'Two-dimensional slope stability analysis by limit equilibrium and strength reduction methods' by YM Cheng, T. Länsivaara and WB Wei", by J. Bojorque, G. DeRoeck J Maertens Comput Geotech 35:309–311

62. ASTM D5199-12 (2019) Standard test method for measuring the nominal thickness of geosynthetics. ASTM Int West Conshohocken, PA. www.astm.org

63. ASTM D5261-10 (2018) Standard test method for measuring mass per unit area of geotextiles. ASTM Int West Conshohocken, PA. www.astm.org

64. ASTM D 4595-17 (2017) Standard test method for tensile properties of geotextiles by the wide-width strip method. ASTM Int West Conshohocken, PA. www.astm.org

65. ASTM D2850-15 (2015) Standard test method for unconsolidated-undrained triaxial compression test on cohesive soils. ASTM Int West Conshohocken, PA. www.astm.org

66. Singh HP (2012) Effects of geogrid sheet on strength and stiffness of loose. Int J Innov Res Sci Eng Technol 2:5290–5299

67. Haeri SM, Noorzad R, Oskoorouchi AM (2000) Effect of geotextile reinforcement on the mechanical behavior of sand. Geotext Geomembr 18:385–402. https://doi.org/10.1016/S0266-1144(00)00005-4

68. Noorzad R, Mirmoradi SH (2010) Laboratory evaluation of the behavior of a geotextile reinforced clay. Geotext Geomembr 28:386–392. https://doi.org/10.1016/j.geotexmem.2009.12.002

69. Tolooiyan A, Abustan I, Selamat MR, Ghaffari S (2009) A comprehensive method for analyzing the effect of geotextile layers on embankment stability. Geotext Geomembr 27:399–405

70. Yang KH, Nguyen MD, Yalew WM et al (2016) Behavior of geotextile-reinforced clay in consolidated-undrained tests: reinterpretation of porewater pressure parameters. J Geoengin 11:45–57. https://doi.org/10.6310/jog.2016.11(2).1

71. Fabian K, Fourie A (1986) Performance of geotextile-reinforced clay samples in undrained triaxial tests. Geotext Geomembr 4:53–63. https://doi.org/10.1016/0266-1144(86)90036-1

72. Yang K-H, Yalew WM, Nguyen MD (2016) Behavior of geotextile-reinforced clay with a coarse material sandwich technique under unconsolidated-undrained triaxial compression. Int J Geomech 16:04015083. https://doi.org/10.1061/(asce)gm.1943-5622.0000611

73. Ingold TS, Miller KS (1982) The performance of impermeable and permeable reinforcement in clay subject to undrained loading. Q J Eng Geol 15:201–208. https://doi.org/10.1144/gsl.qjeg.1982.015.03.03

74. Unnikrishnan N, Rajagopal K, Krishnaswamy NR (2002) Behaviour of reinforced clay under monotonic and cyclic loading. Geotext Geomembr 20:117–133. https://doi.org/10.1016/S0266-1144(02)00003-1

75. Asakereh A, Tafreshi SNM (2007) Strength evaluation of wet reinforced silty sand by triaxial test. Int J Civ Eng 5:273–284

76. Guido VA, Chang DK, Sweeney MA (1986) Comparison of geogrid and geotextile reinforced earth slabs. Can Geotech J 23:435–440. https://doi.org/10.1139/t86-073

77. Nair AM, Latha GM (2014) Large diameter triaxial tests on geosynthetic-reinforced granular subbases. J Mater Civ Eng 27:1–8. https://doi.org/10.1061/(ASCE)MT.1943-5533.0001088

78. Eldesouky HM, Morsy MM, Mansour MF (2016) Fiber-reinforced sand strength and dilation characteristics. Ain Shams Eng J 7:517–526. https://doi.org/10.1016/j.asej.2015.06.003

79. Jewell RA, Milligan GWE, Sarsby RW, Dubois D (1984) Interaction between soil and geogrids. In: Proceedings of symposium on polymer grid reinforcement in civil engineering, London, no 1.3. pp 18–30

80. Sreelakshmi KR, Vasudevan AK (2021) Study on performance of geotextile reinforced soils using triaxial compression test. In: Patel S, Solanki CH, Reddy KR, Shukla SK (eds) BT - proceedings of the indian geotechnical conference 2019. Springer, Singapore. pp 189–200

81. Hassan W, Kanwal M, Nawaz MN, Shahzad A (2021) A comparative study on shear strength characteristics of geotextile reinforced soils. In: Hodja Akhmet Yassawi 4th international conference on scientific research, February 12–13. Ankara, Turkey

82. Schlosser F, Long N-T (1974) Recent results of french research on reinforced earth. J Constr Div 100:223–237. https://doi.org/10.1061/jcceaz.0000429

83. Yang Z, Singh A (1974) Strength and deformation characteristics of reinforced sand. In: International meeting on water resources engineering Los, Angeles, CA

84. Yang Z (1972) Strength and deformation characteristics of reinforced sand. PhD. Thesis, University of California at Los Angeles, Los Angeles, CA

85. Iwamoto MK (2014) Observations from load tests on geosynthetic reinforced soil. Master Thesis, University of Hawai'i at Mānoa, USA

86. Namjoo AM, Soltani F, Toufigh V (2021) Effects of moisture on the mechanical behavior of sand–geogrid: an experimental investigation. Int J Geosynth Gr Eng 7:1–13. https://doi.org/10.1007/s40891-020-00243-w

87. Fourie AB, Fabian KJ (1987) Laboratory determination of clay-geotextile interaction. Geotext Geomembr 6:275–294. https://doi.org/10.1016/0266-1144(87)90009-4

88. Luo N, Bathurst RJ, Javankhoshdel S (2016) Probabilistic stability analysis of simple reinforced slopes by finite element method. Comput Geotech 77:45–55

89. Wei WB, Cheng YM (2010) Soil nailed slope by strength reduction and limit equilibrium methods. Comput Geotech 37:602–618

90. Nasvi MCM, Krishnya S (2019) Stability analysis of Colombo-Katunayake Expressway (CKE) using finite element and limit equilibrium methods. Indian Geotech J 49:620–634